First-principles study of ballistic transport properties in $Co_2MnSi/X/Co_2MnSi(001)$ (X = Ag, Au, Al, V, Cr) trilayers

Yoshio Miura, Koichi Futatsukawa, Shohei Nakajima, Kazutaka Abe, and Masafumi Shirai
Research Institute of Electrical Communication, Tohoku University, Katahira 2-1-1, Aoba-ku, Sendai 980-8577, Japan
(Received 1 August 2011; revised manuscript received 26 September 2011; published 20 October 2011)

We investigate and discuss the origin of interface resistance in magnetic trilayers with the half-metallic Co_2MnSi by performing first-principles electronic-structure and ballistic transport calculations for $Co_2MnSi/X/Co_2MnSi(001)$ (X = Ag, Au, Al, V, Cr). We found that the matching of the Fermi surface projected to the two-dimensional Brillouin zone of in-plane wave vector ($k_\parallel$) is a main contributing factor for the spacer (X) dependence of the interfacial resistance. Furthermore, the MnSi-terminated interface shows low resistance compared with the Co-terminated interface because the Co-terminated interface has a larger d component in the local density of states at the Fermi level than that of the MnSi-terminated interface. We conclude that Ag, Au, and Al spacers with MnSi termination of CMS/X/CMS trilayers will provide the large interfacial spin-asymmetry coefficient because of the small interface resistance in parallel magnetization.

DOI: 10.1103/PhysRevB.84.134432 PACS number(s): 85.75.Bb, 73.43.Qt, 73.20.At

I. INTRODUCTION

The spin-dependent tunneling between two ferromagnetic electrodes separated by a nonmagnetic layer provides the magnetoresistance depending on relative magnetization directions of the ferromagnetic electrodes.[1–3] The effect is essential for applications of spintronics, such as the magnetoresistive random access memory (MRAM) and the read-out head of hard disk drives (HDD). On the tunneling magnetoresistive (TMR) devices, recent development of the magnetic tunnel junctions (MTJs) with the single-crystalline MgO and body-centered-cubic (bcc) Fe(Co) (Refs. 4–6) opens a possibility to realize a high speed and an ultrahigh density for the spintronics applications. In the Fe/MgO/Fe(001) MTJ, the momentum of electrons parallel to the layer $k_\parallel = (k_x, k_y)$ is conserved owing to the two-dimensional (2D) periodicity of the system,[7,8] and electrons with $k_\parallel = (0,0)$ (normal incidence with respect to the plane) dominate the tunneling as is seen for the tunneling of free electrons through a simple square barrier. Furthermore, the tunneling conductance depends strongly on the symmetry of the Bloch states in the electrode, providing effectively slow decay of the evanescent states with Δ_1 symmetry in the barrier layer. Since the bcc Fe and FeCo is half-metallic on the Δ_1 state at $k_\parallel = (0,0)$ around the Fermi level, the Fe/MgO/Fe(001) MTJs have spin-dependent potential in their resistance, leading to a much larger TMR ratio of over 1000% at low temperature. These results indicate that, in the TMR devices, the spin dependence of the current can be characterized by the spin polarization of the Δ_1 state of ferromagnetic electrodes rather than that of total density of states (DOSs) around the Fermi level.

On the other hand, in current-perpendicular-to-plane (CPP) giant magnetoresistive (GMR) devices, a spin-dependent transport can be characterized by the spin polarization of total DOSs of the ferromagnetic layer because, in an all-metallic system, electrons not only with $k_\parallel = (0,0)$ but also with $k_\parallel \neq (0,0)$ can contribute equally to the current. In this case, half-metallic ferromagnets (HMFs), which are metallic for the majority-spin band and semiconducting for the minority-spin band leading to complete (100%) spin polarization at the Fermi level, are important for obtaining the large GMR effects. Among the many theoretically predicted HMFs,[9–14] the Co-based full Heusler alloys Co_2YZ (YZ = MnSi, MnGe, MnAl, FeSi, FeAl) are the most promising candidates for use in spintronics devices owing to their high Curie temperatures above room temperature[16] (RT) and robustness of high spin polarization against atomic disorder.[17–20] So far, the CPP-GMR devices on the basis of the half-metallic Co_2YZ have been fabricated, and the GMR ratio at room temperature has been observed for $Co_2MnSi/Cr/Co_2MnSi$,[21] $Co_2MnSi/Cu/Co_2MnSi$,[22] $Co_2MnSi/Ag/Co_2MnSi$,[23] $Co_2Fe(Al,Si)/Ag/Co_2Fe(Al,Si)$,[25] and $Co_2MnGe/Cu/Co_2MnGe$.[26] Although the observed magnetoresistive effects in CPP-GMR devices are rather small compared with those in TMR devices, studies on the CPP-GMR system are still important because of the small resistance area product (RA), which is crucial for realization of an ultra-high-speed reading in magnetic read heads of HDD.

According to Valet and Fert's two-current model,[15] the resistance change area product between parallel and antiparallel magnetization configurations ($\Delta RA = R_{AP}A - R_P A$) can be expressed by two intrinsic factors on spin-dependent electron scattering. They are the bulk spin-asymmetry coefficient (β) in ferromagnetic (FM) layers and the interfacial spin-asymmetry coefficient (γ). The β is enhanced by using the HMF in the FM layer, while enhancement of the γ is accomplished by reduction of the interface resistance $R_{FM/NM}$ through the choice of nonferromagnetic (NM) spacers. In CPP-GMR devices with HMFs, a matching of the majority-spin band dispersions with the NM spacer is important to reduce the $R_{FM/NM}$. In fact, the large γ has been reported experimentally in the $Co_2MnSi/Ag/Co_2MnSi(001)$ compared with that in the $Co_2MnSi/Cr/Co_2MnSi(001)$,[24] which was attributed to the smaller resistance of the $Co_2MnSi/Ag(001)$ interface than that of the $Co_2MnSi/Cr(001)$ interface. So far, a spin-dependent interface resistance has been investigated for various combinations of FM (Fe, Co, Ni) and NM (Au, Pt, Ag, Cu, Cr) layers. However, the $R_{FM/NM}$ between half-metallic Co_2YZ and NM layers has not yet been discussed, and the microscopic origin

depending on the matching of energy band dispersions and the interfacial structures of each layer is still unclear.

In this paper, we perform first-principles electronic-structure and ballistic transport calculations in order to clarify the origin of interfacial resistance in $Co_2MnSi/X/Co_2MnSi$ (X = Au, Ag, Al, Cr, V) magnetic trilayers. First, we determine stable interfacial structures of $Co_2MnSi/X(001)$ junctions by comparing the formation energy between the Co termination and the MnSi termination for various NM spacers X. We will show that MnSi-terminated interfaces are thermodynamically stable as compared with Co-terminated interfaces, irrespective of NM layers. Then, we calculate the majority-spin transmittance of $Co_2MnSi/X/Co_2MnSi(001)$ trilayers in the parallel magnetization configuration on the basis of the Landauer formula, and discuss the majority-spin interface resistance depending on the NM spacers. We found that the matching of the Fermi surface projected to the two-dimensional Brillouin zone (BZ) in the in-plane wave vector $k_\parallel$ between the Co_2MnSi and NM spacers is a main contributing factor for the interfacial resistance among each spacer. Finally, we discuss the origin of the interface resistance owing to the different terminated interface in the $Co_2MnSi/X/Co_2MnSi(001)$.

II. COMPUTATIONAL METHOD

We perform first-principles calculations for supercells consisting of Co_2MnSi and the NM spacer X (X = Au, Ag, Al, Cr, V) using the density functional theory within the generalized-gradient approximation for the exchange-correlation energy.[27] In order to facilitate the structure optimization, which is important for determining the interface structure, we adopt plane-wave basis sets along with the ultrasoft pseudopotential method by using the quantum code ESPRESSO.[28] The number of **k** points is taken to be $10 \times 10 \times 1$ for all cases, and Methfessel-Paxton smearing with a broadening parameter of 0.01 (Ryd) is used. The cutoff energy for the wave function and charge density is set to 30 (Ryd) and 300 (Ryd), respectively. These values are large enough to deal with all the elements considered here within the ultrasoft pseudopotential method.

A $Co_2MnSi/X/Co_2MnSi(001)$ trilayer is constructed in a tetragonal supercell, where the in-plane lattice parameter of the supercell is fixed at 3.99 Å, which corresponds to half of the square root of the lattice constant of the bulk Co_2MnSi (5.65 Å). The lattice mismatch for each NM spacer is 2.08% for face-centered-cubic (fcc) Au, 2.26% for fcc Ag, 1.36% for fcc Al, 3.01% for bcc Cr, and 7.26% for bcc V, respectively. The $Co_2YZ/X(001)$ interface has two types of termination on Co_2MnSi, namely, the Co termination and the MnSi termination. We prepare the supercell of the multilayer containing 7 atomic layers of NM spacer X and 17 and 15 atomic layers of Co_2YZ for the Co- and MnSi-terminated interfaces, respectively. Figure 1 schematizes the supercell of the $Co_2MnSi/Cr/Co_2MnSi(001)$ for the MnSi termination. The supercell of the Co termination has two more Co atoms at both sides of the MnSi-terminated junctions.

For transport calculations, we consider an open quantum system consisting of a scattering region corresponding to NM spacers X and a junction with Co_2MnSi attached to left and right semi-infinite electrodes corresponding to bulk Co_2MnSi. Transmittance is obtained by solving the scattering equation with infinite boundary conditions in which the wave function of the scattering region and its derivative are connected to the Bloch states of each electrode.[29] The potential in the scattering equation can be obtained from the self-consistent electronic-structure calculations for the supercell containing a left and a scattering region. We confirmed that five atomic layers of Co_2MnSi between the right edge of the electrode region and the left-hand side of the Co_2MnSi/X interface are enough to represent the shape of the local potential of bulk Co_2MnSi in the electrode region.

Since our system is repeated periodically in the xy plane, and propagating states can be assigned by an in-plane wave vector $k_\parallel = (k_x, k_y)$ index, different $k_\parallel$ do not mix and can be treated separately. Furthermore, our approach neglects the spin-orbit interaction and noncollinear spin configuration. Thus, we solve scattering equations for some fixed $k_\parallel$ and spin index on the basis of the approach by Choi and Ihm.[29,30]

As is discussed in Ref. 24, the transport properties obtained from the Landauer formula do not give a real conductance for the three-dimensional metallic multilayer. However, our aim in this paper is not to obtain the quantitatively correct conductance and resistance of ferromagnetic/nonferromagnetic/ferromagnetic(F/N/F) trilayers, but to clarify the difference of the conductance thorough F/N junctions (or interfacial resistance) depending on the nonferromagnetic spacer and the interfacial termination. Since the electrode region (ferromagnetic layer) consists of Co_2MnSi for all cases, the difference of the resistance between F/N/F and F/N′/F trilayers indicates the difference of the interfacial resistance between the F/N and F/N′ junctions, which can be originated from electron scattering due to the change of the local potential and band structures at the interfacial region. Furthermore, we assume the completely epitaxial multilayer, where the crystal momentum parallel to the layer (or $k_\parallel$) is conserved because of the two-dimensional periodicity of the system, and the number of conductive channels perpendicular to plane is less than about five or six per $k_\parallel$. Therefore, the ballistic transport calculations from the Landauer formula can be applied to evaluate the difference of the interfacial resistance depending on the band structures of the materials on both sides of the interface. We have already confirmed this point in our previous work in Ref. 24, where the difference of resistance area product in the ballistic transport calculation between $Co_2MnSi/Cr/Co_2MnSi(001)$ and $Co_2MnSi/Ag/Co_2MnSi(001)$ trilayers is almost comparable to the experimental one. We consider that this justifies the use of Landauer formula for the investigation of the interfacial resistance of all metallic multilayers depending on the nonferromagnetic spacer and the interfacial termination.

III. RESULTS AND DISCUSSION

A. Interfacial structure of $Co_2MnSi/X(001)$

In order to determine the stable interfacial structures for each termination of $Co_2MnSi/X(001)$ junctions, we minimized the total energy by relaxing atomic positions with changing the longitudinal size of the supercell. We found that the interface structure where X atoms are positioned on the hollow site of the Co_2MnSi surface is more stable

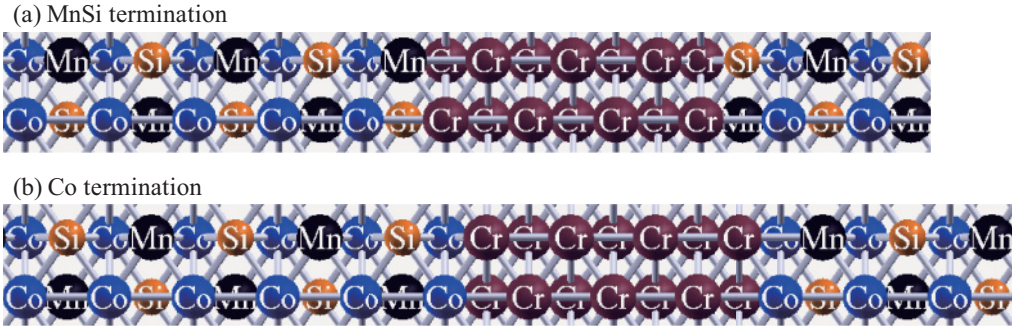

FIG. 1. (Color online) A supercell of the $Co_2MnSi/Cr/Co_2MnSi(001)$ with MnSi termination (upper) and Co termination (lower).

than that of the on-top site both in the Co and MnSi terminations. The $Co_2YZ/Cr(001)$ interfacial structures after the relaxations are schematized in Fig. 1 for both terminations. Then, we calculated the formation energy of these interfaces to determine the relative stability between the Co and MnSi terminations. The formation energy of each termination is given by

$$E_{\rm form}^{\rm term} = E_{\rm tot}^{\rm term} - \sum_i N_i \mu_i, \qquad (1)$$

where $E_{\rm tot}^{\rm term}$ is the total energy of the supercell for each termination, N_i is the number of atoms of each element, and μ_i are their chemical potentials. At equilibrium, the chemical potential of the constituent atoms can not exceed the corresponding one of the bulk phase, i.e., the upper limit of μ_i can be derived from the bulk total energy per atom. Since each supercell is nonstoichiometric only on the Co atom, the difference of the formation energy between Co and MnSi termination $E_{\rm form}^{\rm diff} = (E_{\rm form}^{\rm Co\text{-}term} - E_{\rm form}^{\rm MnSi\text{-}term})/2$ can be expressed as a function of $\mu_{\rm Co}$ only. Furthermore, assuming the thermodynamic equilibrium condition $\mu_{\rm Co_2MnSi} = 2\mu_{\rm Co} + \mu_{\rm Mn} + \mu_{\rm Si}$ and taking $\mu_{\rm Co_2MnSi}$ from the bulk structure, we can determine the lower limit of $\mu_{\rm Co}$ as $\mu_{\rm Co} \geqslant \mu_{\rm Co_2MnSi} - \mu_{\rm Mn(bulk)} - \mu_{\rm Si(bulk)}$, i.e., the formation energy difference is expressed within the thermodynamically allowed range $\mu_{\rm Co_2MnSi} - \mu_{\rm Mn(bulk)} - \mu_{\rm Si(bulk)} \leqslant \mu_{\rm Co} \leqslant \mu_{\rm Co(bulk)}$. It is conventional to refer to the upper limit of $\mu_{\rm Co}$ as the Co-rich limit with $\mu_{\rm Co(hcp-Co)}$.

Table I shows the $E_{\rm form}^{\rm diff}$ (eV/cell area) for the $Co_2MnSi/X(001)$ junctions for the Co-poor and Co-rich limit. The positive (negative) value of $E_{\rm form}^{\rm diff}$ indicates that the MnSi-terminated interface is more stable than the Co-terminated interface, irrespective of the $\mu_{\rm Co}$. We consider that the relaxations of atomic positions in the MnSi-terminated interfaces significantly reduce the formation energy of the supercell.

TABLE I. The formation energy difference between the Co- and MnSi-terminated interface $E_{\rm form}^{\rm diff}$ for the Co-rich and Co-poor limit for $Co_2MnSi/X(001)$ (X = Au, Ag, Al, V, and Cr). The positive (negative) value of $E_{\rm form}^{\rm diff}$ indicates that the MnSi-terminated interface is more (less) stable than the Co-terminated interface.

$E_{\rm form}^{\rm diff}$ (eV/cell area)	Au	Ag	Al	V	Cr
Co-poor	0.381	0.482	0.0806	0.269	0.384
Co-rich	0.249	0.351	−0.0510	0.137	0.252

B. Comparison of the transmittance for $Co_2MnSi/X/Co_2MnSi(001)$

Figure 2 shows majority-spin transmittance in $G_0 = e^2/h$ unit averaged over the two-dimensional Brillouin zone of the in-plane wave vector $k_\parallel$ of $Co_2MnSi/X/Co_2MnSi(001)$ trilayers with the MnSi termination and the Co termination for nonmagnetic spacer X = fcc Au, fcc Ag, fcc Al, bcc V, and antiferromagnetic bcc Cr in a parallel magnetization configuration. First, it is found in Fig. 2 that the averaged transmittance of the trilayer with X = Au, Ag, Al, and V is about $1 \pm 0.2\ G_0$, indicating that each $k_\parallel$ channel has $1G_0$ transmittance on average. On the other hand, the trilayer with antiferromagnetic bcc Cr spacer is about $0.2 \sim 0.3G_0$, which is $1/5 \sim 1/3$ or smaller than that with the other spacer. These results qualitatively agree with recent experimental results on CPP-GMR devices of epitaxial $Co_2MnSi/Ag/Co_2MnSi$ and $Co_2MnSi/Cr/Co_2MnSi$ trilayers, where a smaller resistance area product of the $Co_2MnSi/Ag(001)$ interface than that of the $Co_2MnSi/Cr(001)$ has been obtained.

To look at the ballistic transport properties with a little more detail, we show in Fig. 3 the energy dependence of the transmittance at $k_\parallel = (0,0)$ for the $Co_2MnSi/Ag/Co_2MnSi(001)$ and the $Co_2MnSi/Cr/Co_2MnSi(001)$ with MnSi termination in the parallel magnetization, as a representative case. The band structures of majority-spin Co_2MnSi, fcc Ag, and bcc

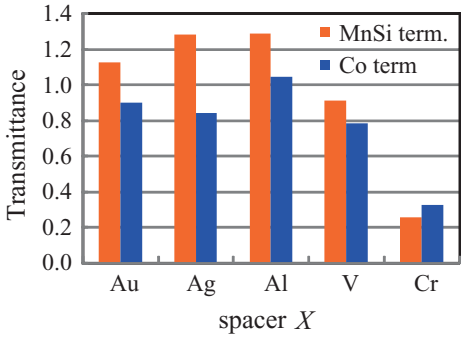

FIG. 2. (Color online) A bar graph to compare the transmittance of $Co_2MnSi/X/Co_2MnSi(001)$ for X = Au, Ag, Al, V, and Cr with MnSi termination and Co termination.

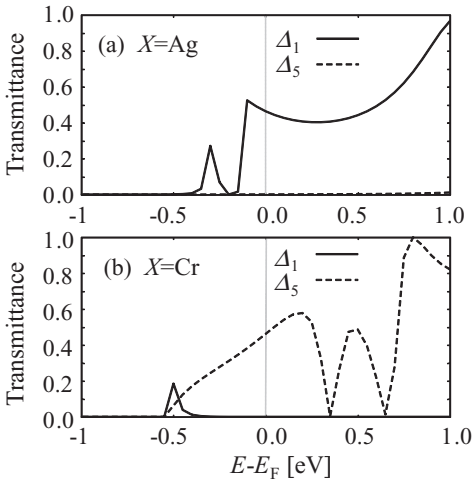

FIG. 3. The majority transmittance as a function of energy at $k_\parallel = (0,0)$ for (a) $Co_2MnSi/Ag/Co_2MnSi(001)$ and (b) $Co_2MnSi/Cr/Co_2MnSi(001)$ trilayers in the parallel magnetization.

Cr along the [001] direction at $k_\parallel = (0,0)$ is presented for comparison in Fig. 4. Although, in the CPP-GMR system, the transport properties can not be determined only by the transmittance at $k_\parallel = (0,0)$, it has great importance to assess band-resolved transmittance for $k_\parallel$ with the high symmetry. From the symmetry analysis of the Co_2MnSi band structure, we found that the lower conduction band in the majority-spin state has the Δ_1 symmetry, while the upper conduction band is doubly degenerate and has the Δ_5 symmetry. On the other hand, fcc Ag has only the Δ_1 band around the Fermi level, while the bcc Cr (antiferromagnetic) has the doubly degenerate Δ_5 bands and a Δ_2 band around the Fermi level. In Fig. 3(a), the Δ_1 channel owing to the lower conduction band of Co_2MnSi dominates the transmittance, indicating the symmetry matching of the Δ_1 wave function in $Co_2MnSi/Ag/Co_2MnSi$, while the transmittance from the Δ_5 channel is three orders of magnitude smaller than that from the Δ_1 channel. In the case of $Co_2MnSi/Cr/Co_2MnSi$ trilayer, on the other hand, the Δ_5 channel dominates the transmittance owing to the band matching. Since the Δ_5 band of Co_2MnSi is doubly degenerate, the total transmittance of the $Co_2MnSi/Cr/Co_2MnSi$ trilayer is

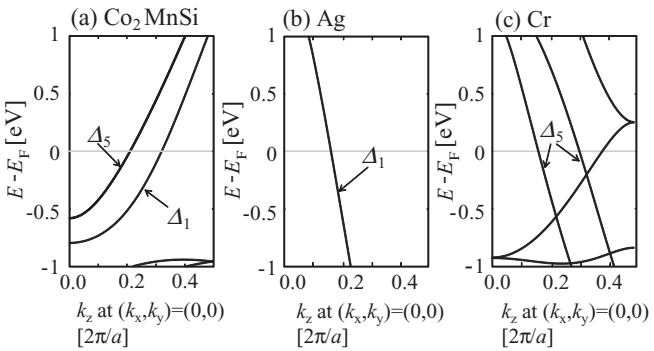

FIG. 4. The majority-spin band structures of bulk (a) Co_2MnSi, (b) fcc Ag, and (c) bcc Cr (antiferromagnetic) along the (001) direction at $k_\parallel = (0,0)$.

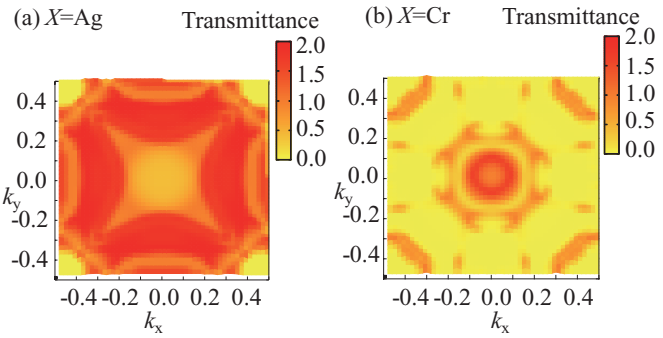

FIG. 5. (Color online) In-plane wave vector $k_\parallel = (k_x, k_y)$ dependence of majority-spin transmittance at the Fermi level for (a) $Co_2MnSi/Ag/Co_2MnSi(001)$ and (b) $Co_2MnSi/Cr/Co_2MnSi(001)$ trilayers in the parallel magnetization.

larger than that of the $Co_2MnSi/Ag/Co_2MnSi$ trilayer at $k_\parallel = (0,0)$. These results indicate that the symmetry matching of the band dispersions between ferromagnetic and NM spacers determines the ballistic transport properties at $k_\parallel = (0,0)$ in an all-metallic multilayer.

We show in Figs. 5(a) and 5(b) the $k_\parallel$ dependence of the majority-spin transmittance at $E = E_F$ in the $Co_2MnSi/Ag/Co_2MnSi$ and $Co_2MnSi/Cr/Co_2MnSi$ trilayers with the MnSi termination in the parallel magnetization. As can be seen in Figs. 5(a) and 5(b), the $k_\parallel$ dependence of the majority-spin transmittance depends strongly on spacer X. The majority-spin transmittance of the $Co_2MnSi/Ag/Co_2MnSi$ trilayers is distributed over the whole 2D $k_\parallel$ BZ, while it is concentrated around $k_\parallel = (0,0)$ and $(\pm 0.5, \pm 0.5)$ in the 2D BZ of the $Co_2MnSi/Cr/Co_2MnSi$ trilayers. The large transmittance at $k_\parallel = (0,0)$ for $X =$ Cr is due to the doubly degenerate Δ_5 band for Co_2MnSi and the antiferromagnetic Cr spacer. These results indicate that the relatively small transmittance in the $Co_2MnSi/Cr/Co_2MnSi$ trilayers can be originated from the behavior of the transmittance in the 2D BZ.

Figure 6 shows the projection of the Fermi surface of bulk Co_2MnSi, fcc Ag, and bcc Cr on the 2D BZ of the (001) face. We found that the $k_\parallel$ dependence of the majority-spin transmittance at $E = E_F$ for the $Co_2MnSi/Ag/Co_2MnSi$ and $Co_2MnSi/Cr/Co_2MnSi$ trilayers can be characterized by the projected Fermi surface of the electrode (Co_2MnSi)

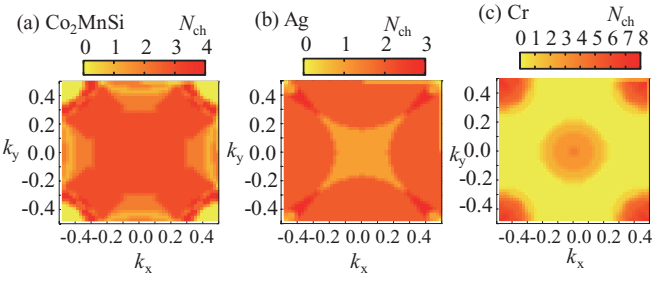

FIG. 6. (Color online) The projection of Fermi surfaces onto the two-dimensional Brillouin zones of in-plane wave vector $k_\parallel = (k_x, k_y)$ for (a) $L2_1$ Co_2MnSi, (b) fcc Ag, and (c) bcc Cr (antiferromagnetic) with the tetragonal unit cell.

and the spacer (Ag or Cr). The large transmittance of the $Co_2MnSi/Ag/Co_2MnSi$ trilayer can be attributed to the large overlapping area of the projected Fermi surface between Co_2MnSi and Ag, while the small overlapping area between Co_2MnSi and Cr in the projected Fermi surface causes small transmittance in the $Co_2MnSi/Cr/Co_2MnSi$ trilayer. These results indicate that the matching of the Fermi surface projected to the two-dimensional Brillouin zone of the in-plane wave vector $k_\parallel$ between the electrode and the spacer is a main contributing factor for the spacer (X) dependence of the transmittance (rather than the matching of the band dispersion at the peculiar k points along the high-symmetry line) in the CPP-GMR system.

C. Interfacial dependence of the transmittance of $Co_2MnSi/X/Co_2MnSi(001)$

The other feature of the transmittance of $Co_2MnSi/X/Co_2MnSi(001)$ shown in Fig. 1 is the interface-structure dependence, i.e., the transmittance of the MnSi termination is larger than that with the Co termination, except for the antiferromagnetic bcc Cr spacer. Analyzing the $k_\parallel$ dependence of the majority-spin transmittance at $E = E_F$ for $Co_2MnSi/X/Co_2MnSi$ trilayers with Co and MnSi termination, we found that the difference

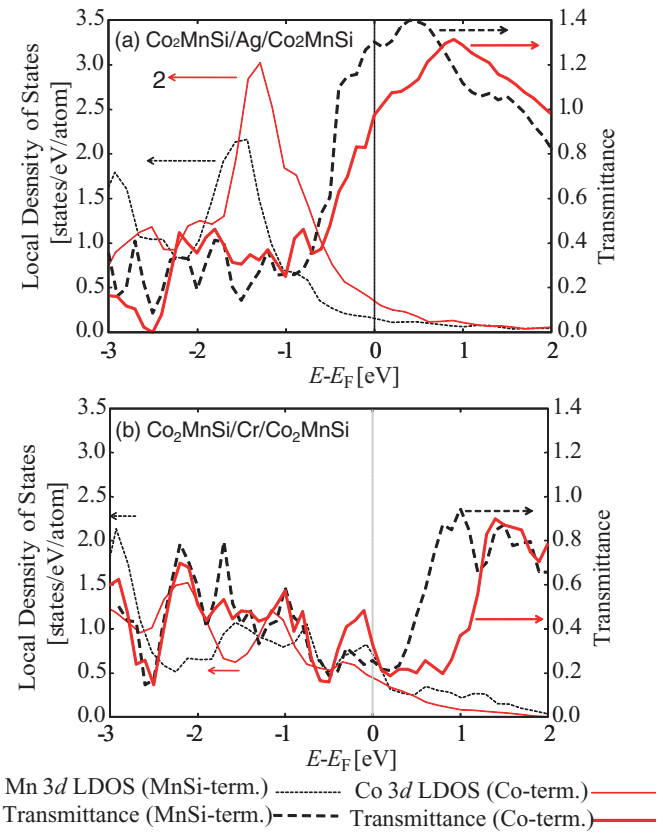

FIG. 7. (Color online) The local density of states (LDOS) of interfacial Co-3d at Co-terminated interface and interfacial Mn-3d at MnSi-terminated interface in (a) $Co_2MnSi/Ag(001)$ and (b) $Co_2MnSi/Cr(001)$, together with the transmittance averaged over the whole $k_\parallel$ region as a function of the energy relative to the Fermi energy.

of the transmittance between two terminations is significant at $k_x \neq 0$ especially for X = Ag, Au, Al, and V. This means that the transmittance in the whole $k_\parallel$ region contributes to interface-structure dependence. To understand this, we show in Fig. 7(a) the local density of states (LDOS) of interfacial Co-3d at Co-terminated interface and interfacial Mn-3d at MnSi-terminated interface in $Co_2MnSi/Ag(001)$, together with the transmittance averaged over the whole $k_\parallel$ region as a function of the energy relative to the Fermi energy. We see that the transmittance increases with decreasing the d component of the LDOS of interfacial atoms, indicating that the interfacial d orbitals act as a scatter of electrons. Furthermore, we found that the LDOS of Co-3d at Co termination shows large components compared with those of Mn at MnSi termination at Fermi level. The large d components at the interfacial regions cause additional reflection of propagating electrons, leading to the large interfacial resistance in the metallic multilayer. These features can be observed also in the LDOS of Co_2MnSi/Au, Co_2MnSi/Al, and Co_2MnSi/V interfaces. In Fig. 7(b), however, we can not find clear relation between the LDOS of interfacial d orbital and the transmittance. This can be attributed to the different magnetic coupling between MnSi termination and Co termination at $Co_2MnSi/Cr(001)$ interface. The local spin moment of interfacial Co ferromagnetically couples with that of Cr, while interfacial Mn shows antiferromagnetic coupling with interfacial Cr. This means that the spin-dependent ballistic transport properties of magnetic layer are significantly affected also by the interfacial magnetic coupling, i.e., the ferromagnetic or antiferromagnetic coupling between interfacial atoms

IV. SUMMARY

In this paper, we perform first-principles electronic-structure and ballistic transport calculations in order to clarify the origin of interfacial resistance in $Co_2MnSi/X/Co_2MnSi$ magnetic trilayers, where X is a spacer layer of NM with Au, Ag, Al, V, and Cr. First, we determined stable interfacial structures of $Co_2MnSi/X(001)$ junctions by comparing the formation energy between the Co termination and the MnSi termination for various NM spacers X. We found that MnSi-terminated interfaces are thermodynamically stable as compared with Co-terminated interfaces, irrespective of NM layers because of the relaxation of the interfacial structures. Then, we calculated the majority-spin transmittance of $Co_2MnSi/X/Co_2MnSi(001)$ trilayers in the parallel magnetization configuration on the basis of the Landauer formula, and found that the matching of the Fermi surface projected to the two-dimensional Brillouin zone in the in-plane wave vector $k_\parallel$ between the Co_2MnSi and NM spacers is a main contributing factor for the interfacial resistance among each spacer. Furthermore, we examined the origin of the interface resistance owing to the different terminated interface in the $Co_2MnSi/X/Co_2MnSi(001)$. We found that the interfacial d orbital at the Fermi level causes additional reflection of incident electrons, and the charge distribution around the interfacial Co-3d orbital at the Co-terminated interface decreases the transmittance of the Co termination compared to that of the MnSi termination. All these results indicate that the ballistic transport properties of

the CPP-GMR magnetic layer are significantly affected by the electronic structures at the interface, especially by the position of *d* orbital relative to the Fermi level, and the interfacial magnetic coupling between the ferromagnet-antiferromagnet heterojunctions. We conclude that Ag, Au, and Al spacers with MnSi termination of CMS/X/CMS trilayers will provide the large interfacial spin-asymmetry coefficient because of the small interface resistance in parallel magnetization and are worth further investigation.

ACKNOWLEDGMENTS

We are grateful to K. Inomata of National Institute for Materials Science and Y. Sakuraba of Tohoku University for valuable discussions of our work. This work was supported by a Grant-in-Aid for Scientific Research (Grant Nos. 19048002, 22360014, and 22760003) from MEXT, the Japan Science and Technology (JST) through its Strategic International Cooperative Program under the title Advanced spintronic materials and transport phenomena (ASPIMATT).

[1] M. N. Baibich, J. M. Broto, A. Fert, F. Nguyen Van Dau, F. Petroff, P. Etienne, G. Creuzet, A. Friederich, and J. Chazelas, Phys. Rev. Lett. **61**, 2472 (1988).
[2] G. Binasch, P. Grünberg, F. Saurenbach, and W. Zinn, Phys. Rev. B **39**, 4828 (1989).
[3] T. Miyazaki and N. Tezuka, J. Magn. Magn. Mater. **139**, L231 (1995).
[4] S. Yuasa, T. Nagahama, A. Fukushima, Y. Suzuki, and K. Ando, Nat. Mater. **3**, 868 (2004).
[5] S. S. P. Parkin, C. Kaiser, A. Panchula, P. M. Rice, B. Hughes, M. Samant, and S.-H. Yang, Nat. Mater. **3**, 862 (2004).
[6] S. Ikeda, J. Hayakawa, Y. M. Lee, F. Matsukura, Y. Ohno, T. Hanyu, and H. Ohno, IEEE Trans. Electron Devices **54**, 991 (2007).
[7] W. H. Butler, X.-G. Zhang, T. C. Schulthess, and J. M. MacLaren, Phys. Rev. B **63**, 054416 (2001).
[8] J. Mathon and A. Umerski, Phys. Rev. B **63**, 220403(R) (2001).
[9] R. A. de Groot, F. M. Mueller, P. G. van Engen, and K. H. J. Buschow, Phys. Rev. Lett. **50**, 2024 (1983).
[10] K. Schwarz, J. Phys. F: Met. Phys. **16**, L211 (1986).
[11] W. E. Pickett and D. J. Singh, Phys. Rev. B **53**, 1146 (1996).
[12] S. Ishida, S. Fujii, S. Kashiwagi, and S. Asano, J. Phys. Soc. Jpn. **64**, 2152 (1995).
[13] S. Picozzi, A. Continenza, and A. J. Freeman, Phys. Rev. B **66**, 094421 (2002).
[14] I. Galanakis, P. H. Dederichs, and N. Papanikolaou, Phys. Rev. B **66**, 174429 (2002).
[15] T. Valet and A. Fert, Phys. Rev. B **48**, 7099 (1993).
[16] J. G. Booth, in *Ferromagnetic Materials*, edited by E. P. Wohlfarth and K. H. J. Buschow (Elsevier, Amsterdam, 1988), Vol. 4, pp. 288.
[17] K. Inomata, S. Okamura, R. Goto, and N. Tezuka, Jpn. J. Appl. Phys. **42**, L419 (2003).
[18] Y. Miura, K. Nagao, and M. Shirai, Phys. Rev. B **69**, 144413 (2004); J. Appl. Phys. **95**, 7225 (2004).
[19] S. Picozzi, A. Continenza, and A. J. Freeman, Phys. Rev. B **69**, 094423 (2004).
[20] Y. Miura, M. Shirai, and K. Nagao, J. Appl. Phys. **99**, 08J112 (2006).
[21] K. Yakushiji, K. Saito, S. Mitani, K. Takanashi, Y. K. Takahashi, and K. Hono, Appl. Phys. Lett. **88**, 222504 (2006).
[22] T. Mizuno, Y. Tsuchiya, T. Machita, S. Hara, D. Miyauchi, K. Shimazawa, T. Chou, K. Noguchi, and K. Tagami, IEEE Trans. Magn. **44**, 3584 (2008).
[23] T. Iwase, Y. Sakuraba, S. Bosu, K. Saito, S. Mitani, and K. Takanashi, Appl. Phys. Express **2**, 063003 (2009).
[24] Y. Sakuraba, K. Izumi, T. Iwase, S. Bosu, K. Saito, K. Takanashi, Y. Miura, K. Futatsukawa, K. Abe, and M. Shirai, Phys. Rev. B **82**, 094444 (2010).
[25] Y. K. Takahashi, A. Srinivasan, B. Varaprasad, A. Rajanikanth, N. Hase, T. M. Nakatani, S. Kasai, T. Furubayashi, and K. Hono, Appl. Phys. Lett. **98**, 152501 (2011).
[26] M. J. Carey, S. Maat, S. Chandrashekariaih, J. A. Katine, W. Chen, B. York, and J. R. Childress, J. Appl. Phys. **109**, 093912 (2011).
[27] J. P. Perdew, K. Burke, and M. Ernzerhof, Phys. Rev. Lett. **77**, 3865 (1996).
[28] S. Baroni, A. Dal Corso, S. de Gironcoli, and P. Giannozzi, [http://www.pwscf.org].
[29] H. J. Choi and J. Ihm, Phys. Rev. B **59**, 2267 (1999).
[30] A. Smogunov, A. Dal Corso, and E. Tosatti, Phys. Rev. B **70**, 045417 (2004).